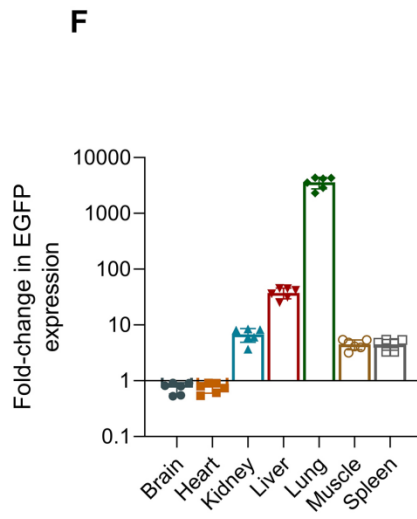
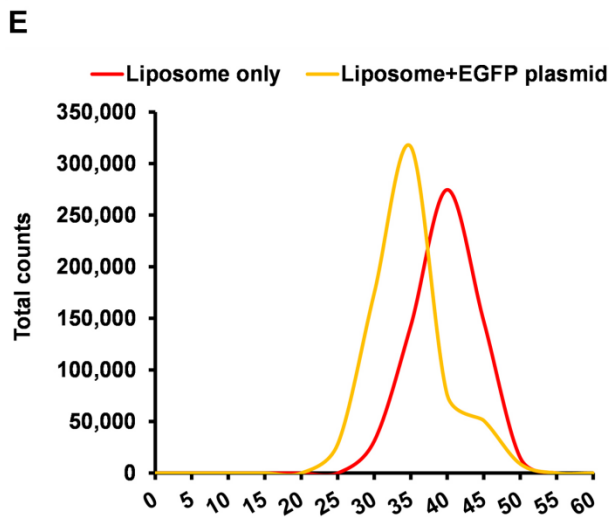
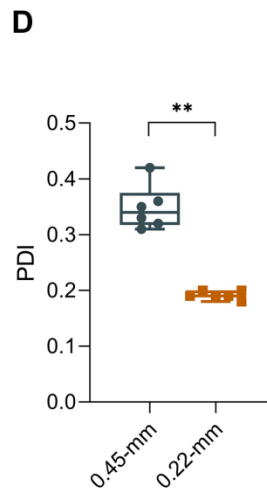
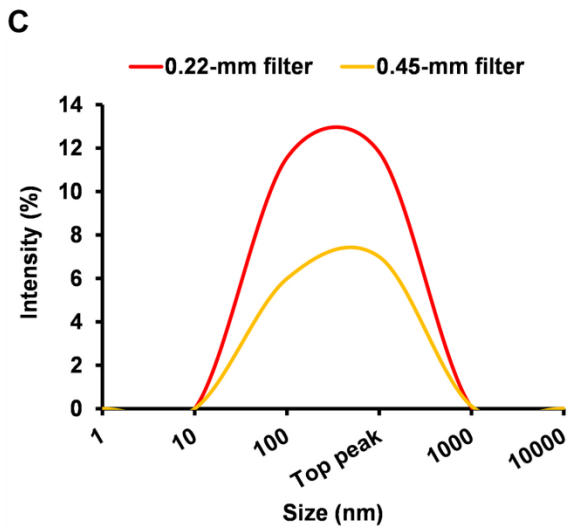
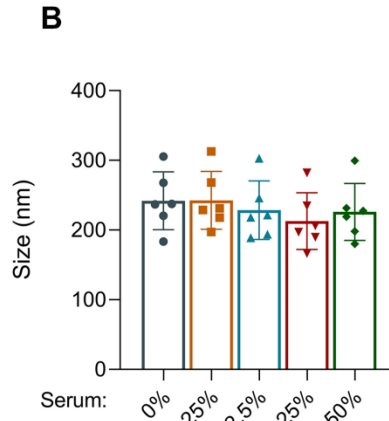
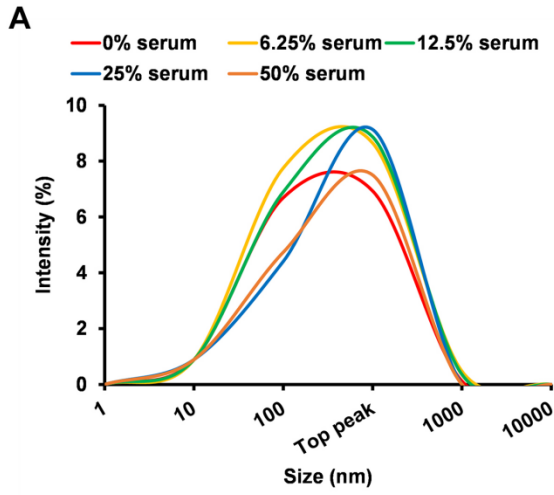


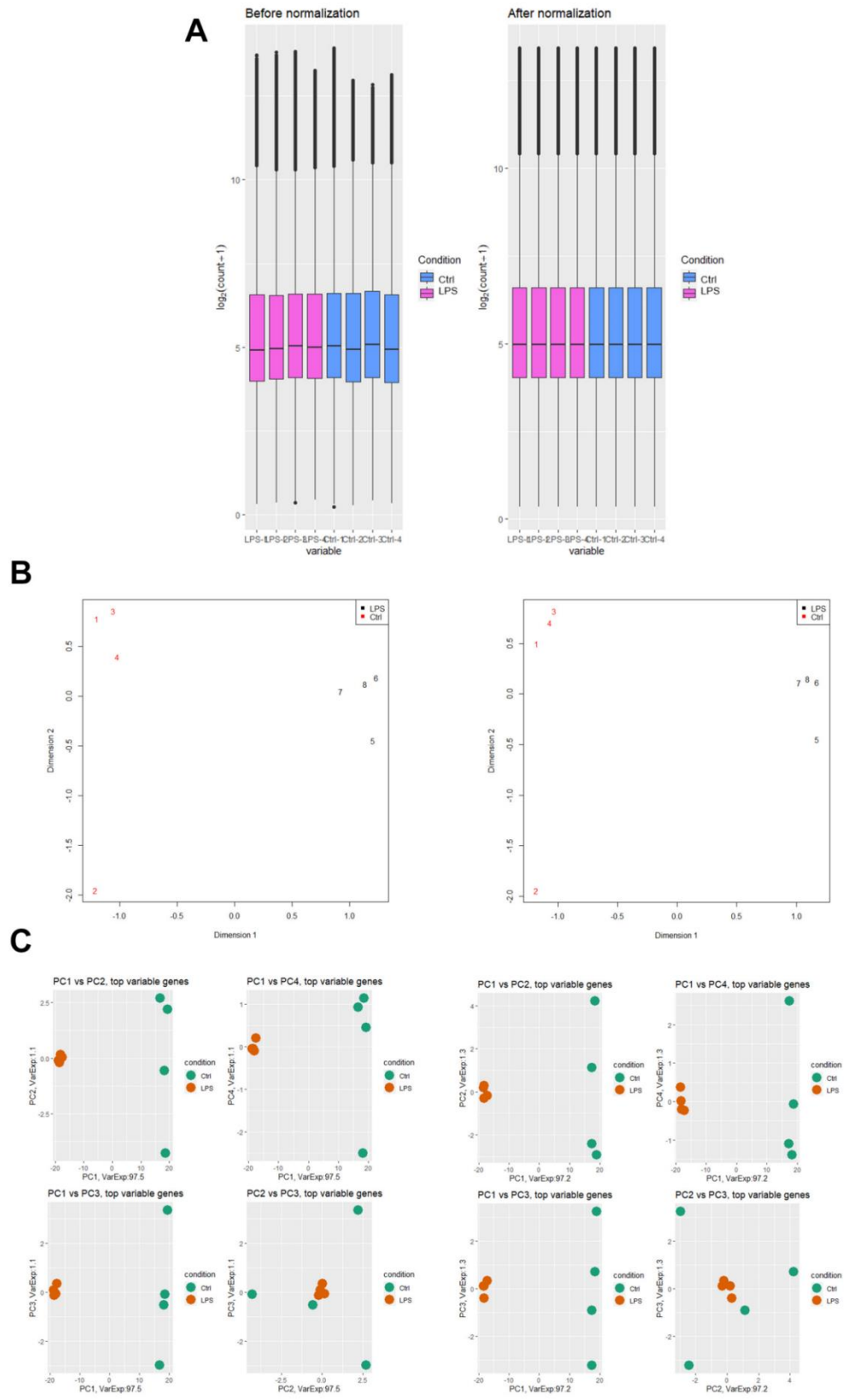
**SUPPLEMENTARY FIGURES**

**Supplementary Figure S1**



**Supplementary Figure S1. Characterization of liposomes.** (A) Following a 2 hour ultracentrifugation, extracellular vesicles were removed from serum and measured for size. Liposomes were prepared through combining liposomes (100  $\mu$ l) and 900- $\mu$ l serum fractions that had been serially-diluted to 50%, 25%, 12.5%, and 6.25% serum. (B) Following a 5-minute incubation, the liposome size was determined by dynamic light scattering. (C) Liposome hydrodynamic diameter was determined using dynamic light scattering following preparation with either a 0.45-mm or 0.22-mm filter and (D) polydispersity index (PDI) distributions of liposomes prepared using a 0.45-mm or 0.22-mm filter. There was a clear narrowing of the PDI distribution when using the 0.22-mm filter. (E) Liposome characterization of zeta potential indicated their cationic nature. The liposome zeta potential reduced following the introduction of plasmid DNA. (F) *EGFP* transgene organ biodistribution following *in vivo* delivery of liposomes. Organs were harvested 23 hours post-liposomal injection. *EGFP* mRNA expression levels assessed by qPCR showed that the lung was the organ with the greatest *EGFP* transgene expression. Data represented as means  $\pm$  SDs. \* $P$ <0.05, \*\* $P$ <0.01 [one-way ANOVA with Dunnett's post-hoc tests].

Supplementary Figure S2

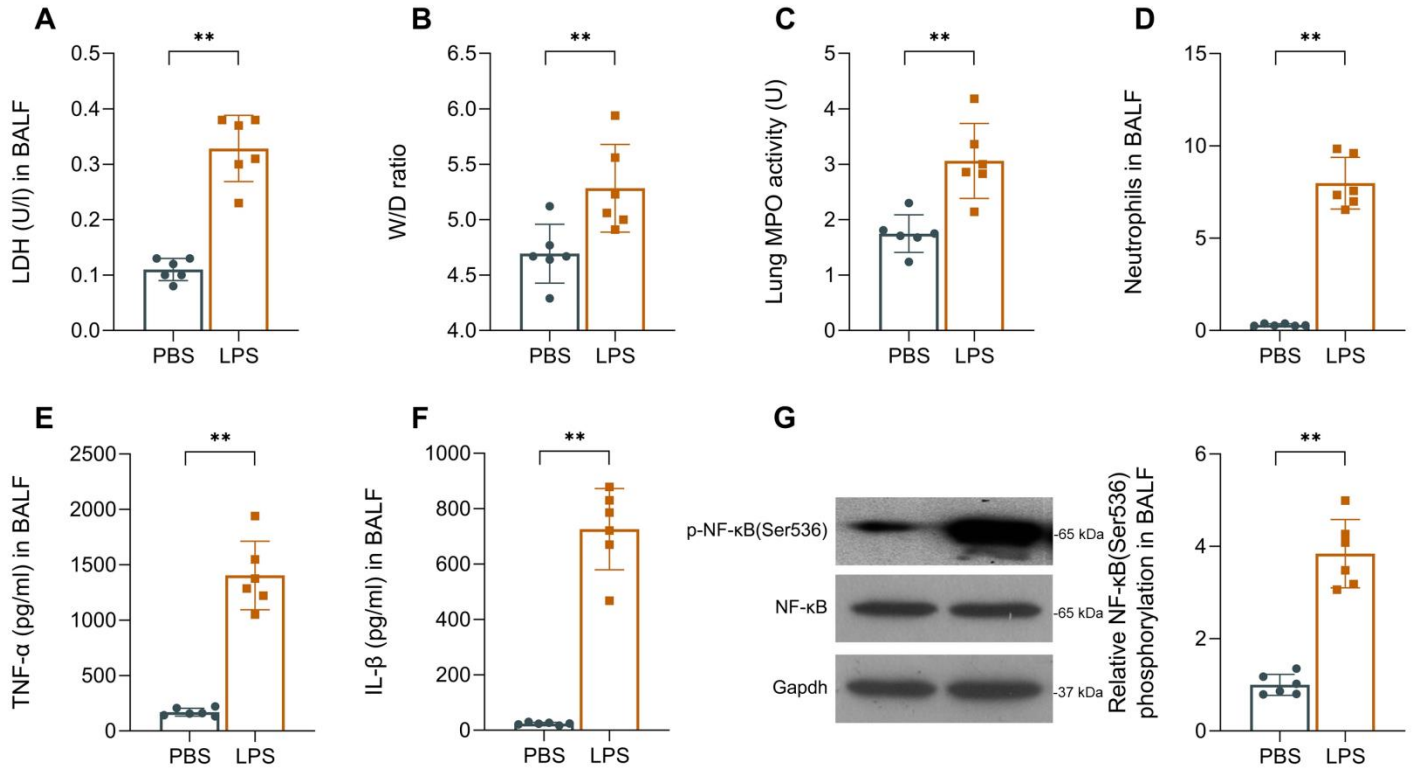


**Supplementary Figure S2. R-based filtering and normalization.** (A) Boxplots of expression data before and after normalization. The post-normalization boxplots distribute in the same intervals with the same median, indicating successful normalization. (B) Multi-dimensional scaling (MDS) plots before and after normalization and (C) principal components analysis (PCA) plots before and after normalization showing clear separation of the experimental groups.



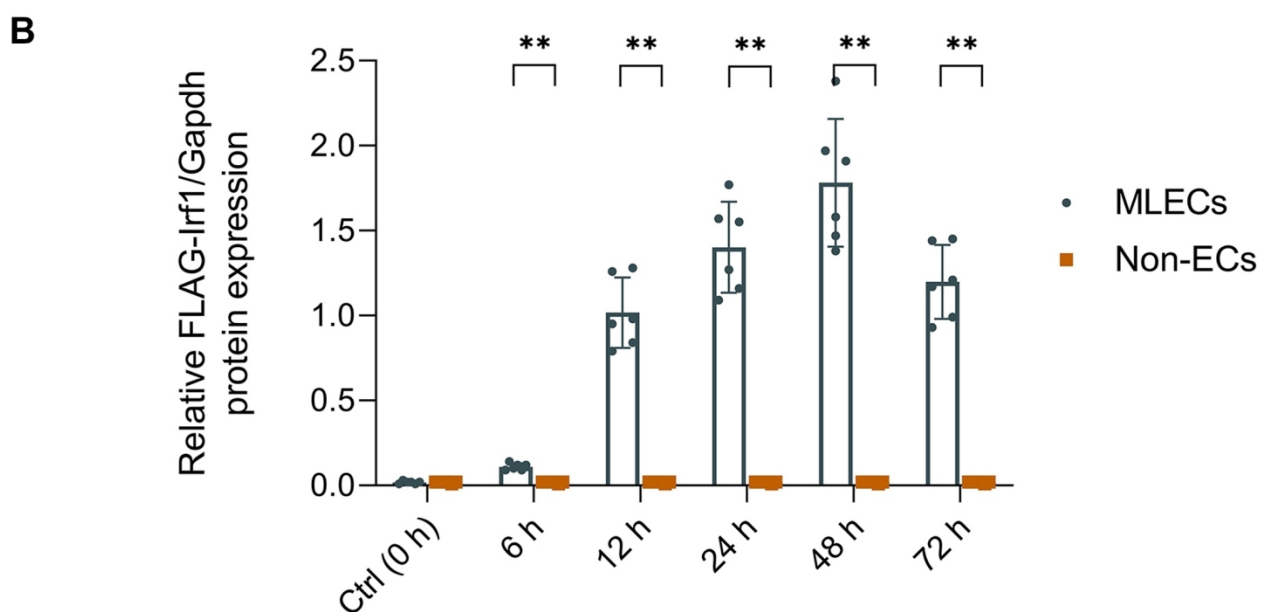
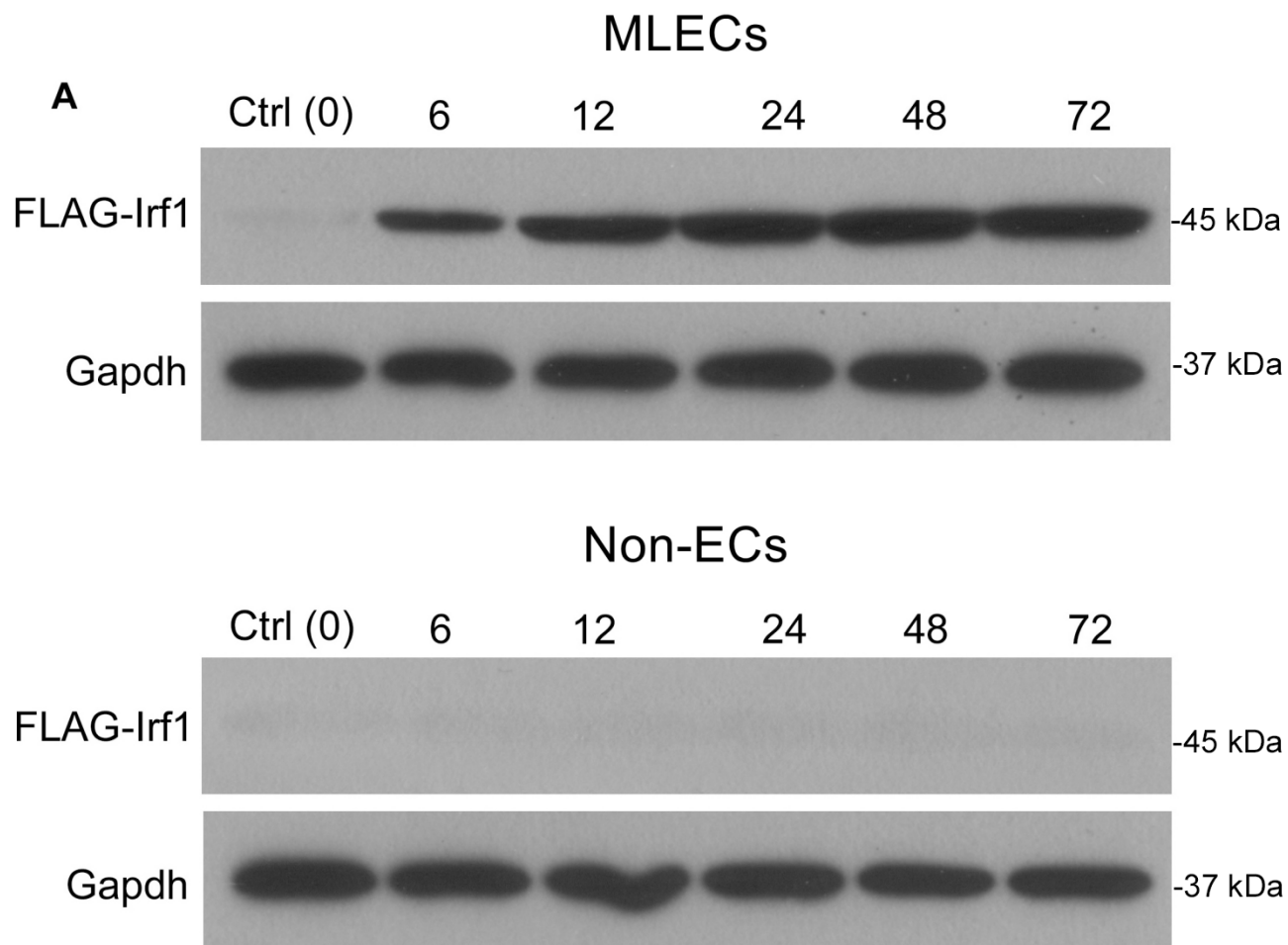
**Supplementary Figure S3. *LIF* promoter analysis.** (A) Schematic of the JASPAR CORE 2016 IRF1 ISRE motif employed in the *LIF* promoter analysis. (B) The 1000-bp promoter segment immediately upstream of the human *LIF* transcription start site (TSS) was analyzed using the ConTra v3 tool to identify putative IRF1 binding sites. One IRF1 ISRE binding site (circled in red) was conserved across multiple species. (C) Detailed sequence of the IRF1 ISRE binding site.

## Supplementary Figure S4



**Supplementary Figure S4. Assessment of lung inflammation in ALI model mice.** Mice were randomly divided into two cohorts ( $n=6$  mice/cohort) and subjected to either i.p. injection of LPS or PBS vehicle control. The following studies were performed 24 h post-injection. Assessment of (A) BALF LDH by ELISA, (B) lung W/D ratio; (C) lung homogenate MPO activity, (D) BALF neutrophil count, (E) BALF TNF- $\alpha$  by ELISA, (F) BALF IL-1 $\beta$  by ELISA, and (G) NF- $\kappa$ B(Ser536) phosphorylation by Western blotting. Data represented as means  $\pm$  SDs. \* $P<0.05$ , \*\* $P<0.01$  [Student's  $t$ -test].

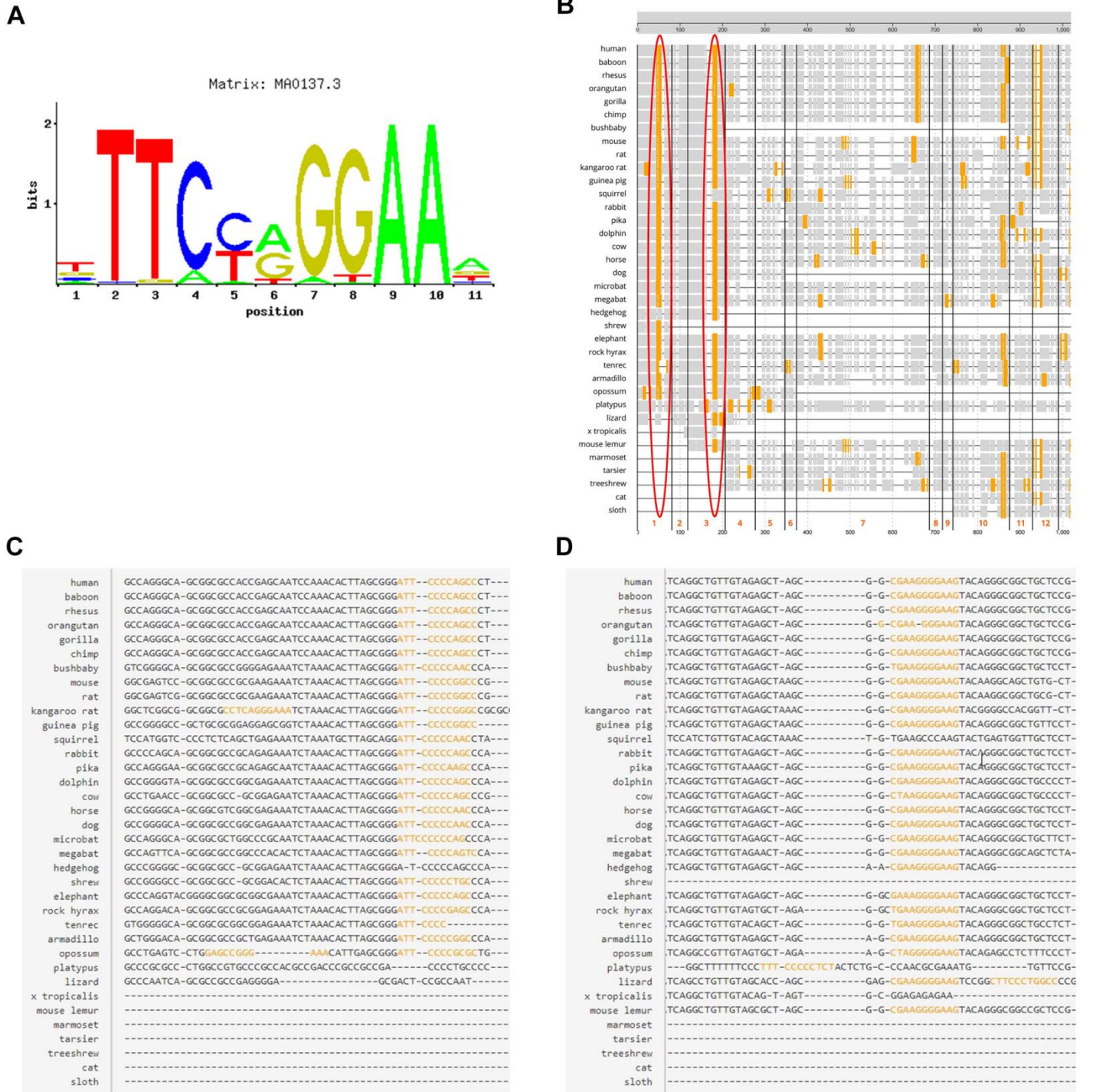
Supplementary Figure S5





**Supplementary Figure S5. Liposomal delivery of endothelial cell-specific FLAG-*Irf1*.** Representative immunoblots and densitometric quantification of FLAG-*Irf1* expression in lung endothelial cells and non-endothelial cells post-LPS at various time points indicated. Data represented as means  $\pm$  SDs. \* $P < 0.05$ , \*\* $P < 0.01$  [two-way ANOVA].

# Supplementary Figure S6



**Supplementary Figure S6. *IRF1* promoter analysis.** (A) Schematic of the JASPAR CORE 2016 STAT1 GAS motif employed in the *IRF1* promoter analysis. (B) The promoter sequence of the human *IRF1* gene was analyzed using the ConTra v3 tool to identify putative STAT1 GAS binding sites. Two STAT1 GAS binding sites (circled in red) were conserved across multiple species. (C, D) Detailed sequences of (C) the STAT1 GAS1 binding site and (D) the STAT1 GAS2 binding site.

## SUPPLEMENTARY TABLES

**Supplementary Table S1. qPCR primer sequences.**

<b>Target</b>	<b>Forward primer (5'→3')</b>	<b>Reverse primer (5'→3')</b>
<i>Lif</i> (murine)	TCAACTGGCACAGCTCAATGGC	GGAAGTCTGTCATGTTAGGCGC
<i>LIF</i> (human)	AGATCAGGAGCCAACTGGCACA	GCCACATAGCTTGTCCAGGTTG
<i>Irf1</i> (murine)	TCCAAGTCCAGCCGAGACACTA	ACTGCTGTGGTCATCAGGTAGG
<i>IRF1</i> (human)	GAGGAGGTGAAAGACCAGAGCA	TAGCATCTCGGCTGGACTTCGA
IRF1 ISRE site on <i>LIF</i> promoter (human)	GTCTGTTCTCCCCACCCTC	ACTGGAGCCTGTGTTGTAAGA
STAT1 GAS1 site on <i>IRF1</i> promoter (human)	GAACAGCCGCGTCTAATTGG	GAAAGCGAAACTACCCGGC
STAT1 GAS2 site on <i>IRF1</i> promoter (human)	CGTCCTTCTGATCGTTCTCTAAG	GTATTTCCGCCGGCTTCC

**Supplementary Table S2. Results from the CemiTool gene set enrichment analysis (GSEA).**

<b>Module</b>	<b>LPS net enrichment score (NES)</b>	<b>Adj. <i>p</i>-value</b>
M1	3.95	0.00069**
M2	4.89	0.00069**
M3	0.88	0.73851

\* $P < 0.05$ , \*\* $P < 0.01$

**Supplementary Table S3. Total body weights for mouse cohorts in the pulmonary transvascular permeability assays (means  $\pm$  SDs).**

<b>(A)</b>	<i>Irf1</i> <sup>fl/fl</sup> Ctrl	<i>Irf1</i> <sup>EC-/-</sup>		<i>P</i> -value
PBS	23.5 $\pm$ 1.7	22.1 $\pm$ 1.9		0.21
LPS (24 h)	22.1 $\pm$ 1.3	21.5 $\pm$ 1.5		0.41
LPS (72 h)	20.3 $\pm$ 0.8	20.0 $\pm$ 0.7		0.44
LPS (120 h)	20.6 $\pm$ 1.2	20.3 $\pm$ 1.6		0.74
<b>(B)</b>	<i>Irf1</i> <sup>EC-/-</sup> pcDNA-Ctrl	<i>Irf1</i> <sup>EC-/-</sup> pcDNA- <i>Irf1</i>		<i>P</i> -value
PBS	23.6 $\pm$ 2.7	21.7 $\pm$ 1.6		0.18
LPS (72 h)	18.7 $\pm$ 1.3	19.5 $\pm$ 1.0		0.29
LPS (120 h)	21.7 $\pm$ 1.9	19.5 $\pm$ 2.8		0.15
<b>(C)</b>	pcDNA-Ctrl	pcDNA- <i>Irf1</i>	pcDNA- <i>Irf1</i> /shLif	<i>P</i> -value
PBS	21.5 $\pm$ 2.1	20.8 $\pm$ 1.6	21.1 $\pm$ 1.7	0.80
LPS (24 h)	22.8 $\pm$ 2.0	22.0 $\pm$ 2.7	23.0 $\pm$ 2.4	0.75
LPS (72 h)	20.1 $\pm$ 1.7	19.4 $\pm$ 1.7	20.0 $\pm$ 1.3	0.71
LPS (120 h)	23.8 $\pm$ 2.7	22.1 $\pm$ 2.2	23.5 $\pm$ 1.9	0.41